Qualitative analysis of geophysical anomalies and seismicity in Mexico: An integrated mapping by GMT

Polina Lemenkova

BOLETIM DE GEOGRAFIA
ISSN: 2176-4786 | DGE - EDUEM - UEM | http://www.periodicos.uem.br/ojs/index.php/BolGeogr/index
DOI: https://doi.org/10.4025/bolgeogr.v39.a2021.e60474 | Submissão: 08-08-2021 | Aceite: 15-12-2021

Qualitative analysis of geophysical anomalies and seismicity in Mexico: An integrated mapping by GMT

Análise qualitativa de anomalias geofísicas e sismicidade no México: um mapeamento integrado por GMT

Polina Lemenkova
Université Libre de Bruxelles, Brussels, Brussels-Capital Region, Belgium
pauline.lemenkova@gmail.com
ORCID: https://orcid.org/0000-0002-5759-1089

ABSTRACT

Geophysical data from open sources are widely used as support of integrated analysis in regional geologic studies in seismically active areas, such as Mexico. High seismicity with repetitive earthquakes occurs in areas of the subduction zones formed during the tectonic evolution and correlates with geophysical anomalous fields. This paper investigates the correspondence between the geophysical, topographic and seismic setting of Mexico using Generic Mapping Tools (GMT) scripting toolset for data processing. The approach for automated mapping using GMT console and shell scripts is presented as an advanced cartographic method aimed to get insights into in the geology and geophysics of Mexico. The data were obtained from open source high-resolution datasets: GEBCO, EGM-2008, satellite-derived gravity, EMAG2 magnetic anomaly and IRIS seismic database. The correspondence between the geological and geophysical data of Mexico has been verified through the comparison between the thematic maps, regional distribution of gravity anomalies and locations of earthquakes. Seven new maps are performed on geologic, geophysical, topographic and seismic data. Seismic mapping is presented for the period of 2007-2021 demonstrating events with magnitude from 1.5 to 7.2. The impact of tectonic processes that formed Middle American Trench and active Trans-Mexican Volcanic Belt on high regional seismicity with intensive earthquakes is explored. The study finds that GMT is an effective tool for high-quality mapping and cartographic analysis. The IRIS data can be used for geologic analysis of Mexico.

Keywords: Cartography, Geophysics, Earthquakes, Geology, Central America.

RESUMO

Dados geofísicos de fontes abertas são amplamente usados como suporte de análise integrada em estudos geológicos regionais em áreas sismicamente ativas, como o México. Alta sismicidade com terremotos repetitivos ocorre em áreas das zonas de subducção formadas durante a evolução tectônica e se correlaciona com campos anômalos geofísicos. Este artigo investiga a correspondência entre o cenário geofísico, topográfico e sísmico do México usando o conjunto de ferramentas de script Generic Mapping Tools (GMT) para processamento de dados. A abordagem para mapeamento automatizado usando o GMT e scripts de shell é apresentada como um método cartográfico avançado com o objetivo de obter insights sobre a geologia e a geofísica do México. Os dados foram obtidos de conjuntos de dados de alta resolução de código aberto: GEBCO, EGM-2008, gravidade derivada de satélite, anomalia magnética EMAG2 e banco de dados sísmico IRIS. A correspondência entre os dados geológicos e geofísicos do México foi verificada através da comparação entre os mapas temáticos, distribuição regional de anomalias gravitacionais e localizações de terremotos. Sete novos mapas são realizados em dados geológicos, geofísicos, topográficos e sísmicos. O mapeamento sísmico é apresentado para o período de 2007-2021 demonstrando eventos com magnitude de 1,5 a 7,2. O impacto dos processos tectônicos que formaram a trincheira da América Central e o cinturão vulcânico transmexicano ativo na alta sismicidade regional com terremotos intensos é explorado. O estudo concluiu que o GMT é uma ferramenta eficaz para mapeamento e análise cartográfica de alta qualidade. Os dados IRIS podem ser usados para análises geológicas do México.

Palavras-chave: Cartografia, Geofísica, Terremotos, Geologia, América Central.

1. INTRODUCTION

The application of the advanced cartographic scripting methods of GMT enables to achieve twofold cartographic goals: 1) accurate representation of the numerical values of the spatial data (SCHENKE; LEMENKOVA, 2008; LEMENKOVA, 2020d); 2) aesthetics and vision beauty of maps, which was an object of studies itself (TAYLOR, 1985; LERNER *et al.*, 1994; LAVIE *et al.*, 2011; SUETOVA *et al.*, 2005b). Hence, using scripting methods of GMT in cartographic visualization is an approach that considers the questions of design in data visualization, quantitative and qualitative analysis of thematic data (geology, geophysics, seismicity), cartographic projection of spatial data, as well as technical aspects of data visualisation.

The integration of a multi-disciplinary approaches of the GMT-based mapping enabled to identify and highlight correlations between the depicted geographic objects more effectively than in GIS-based mapping using Graphical User Interface (GUI) that mostly uses the pre-defined standards of data visualization and lacks operative scripting. Scripting approach aims to automate the workflow in cartographic modelling and mapping through the machine-based data processing that operates with data and performs mapping using a special syntax of the embedded language similar to the programming (LEMENKOV; LEMENKOVA, 2021b) but applied for cartography.

The goal of this paper is to present an integrated study on geologic, topographic and geophysical setting Mexico using open source data. The data have been visualized using GMT and QGIS, used for data visualization to map the correlations between the geospatial variables and seismicity of the country. Then, the IRIS dataset on earthquakes in Mexico is applied and integrated to the GMT to visualize the distribution of major seismic areas in the country caused by the tectonic activity of the subducting lithosphere plates.

The relevance of this research is explained by its actuality and innovativeness. Currently there are no integrated studies on geology and seismicity of Mexico using GMT and IRIS dataset with explanations of GMT codes aimed at earthquake monitoring of the country in the context of its geologic and topographic setting. This explains a need for new methods in thematic mapping of Mexico based on the open source datasets and novel scripting techniques that would be adapted to the rich and complex geologic setting of Mexico.

The key issues of the present research include the technical use of GMT for quantitative visualization of geological and seismic variables and geophysical grids. For instance, monitoring magnitude and distribution and depth of earthquakes can be effectively used for seismological studies through analysis of visualised IRIS dataset. The advantages of scripting cartography for geological studies of Mexico are demonstrated and a series of new maps are presented that can be reused in relevant studies on the geology and geophysics of Mexico.

2. GEOLOGIC SETTING OF MEXICO

Rich geologic setting of Mexico, its structure and tectonic evolution strongly affected its current topography and formation of landscapes. Major geological features of the country are shown in **Figure 1**. Hence, geological processes in the subduction zone are the major factors that determine landscapes responding to either tectonic or climatic changes through time (GODÍNEZ-TAMAY *et al.*, 2020; CASTILLO, 2021; KUHN *et al.*, 2006; LEMENKOVA, 2021a; CASTILLO *et al.*, 2014). The geomorphological responses may also include, for instance river incision, increased channel steepness in the hydrological network, changes in basin relief, *etc*. More details regarding the geologic evolution of Mexico region is reported in the relevant works (e.g. SOLARI *et al.*, 2013; ARCE *et al.*, 2019, 2020; AGUIRRE-DÍAZ; LÓPEZ-MARTÍNEZ, 2009).

Earthquakes are the main geological disasters that occur in Mexico due to its location in the tectonic plate subduction. The country is situated on the North American tectonic plate, however, the complex interaction pattern with other several plates significantly affect its tectonic setting

(ORTEGA-GUTIÉRREZ; GÓMEZ-TUENA, 2018). Thus, the Pacific Plate slides along the North American Plate (NAP) in NW direction while the Cocos plate subducts under NAP (CALÒ, 2021). The NAP experiences the oblique collision and underthrusting with the Caribbean Plate (RODRÍGUEZ-ZURRUNERO *et al.*, 2019; LEMENKOVA, 2020a; SPIKINGS *et al.*, 2015).

Additionally, two minor plates, the Rivera and the Orozco, subducting under the NAP, contribute to the tectonic complexity of the region causing high geological variability, instability and seismicity in the region (**Figure 1**). The Rivera Plate subducts under the NAP (RODRÍGUEZ-PÉREZ; RAMÓN ZUÑIGA, 2018), and the Orozco Fracture Zone (OFZ) separates segments of the Cocos Plate that differ in age and continues the Middle America Trench (BLATTER; HAMMERSLEY, 2010; LEMENKOVA, 2019a).

Figure 1: Geologic map of Mexico. Mapping: QGIS. Vector data: Padilla y Sánchez *et al.*, 2013

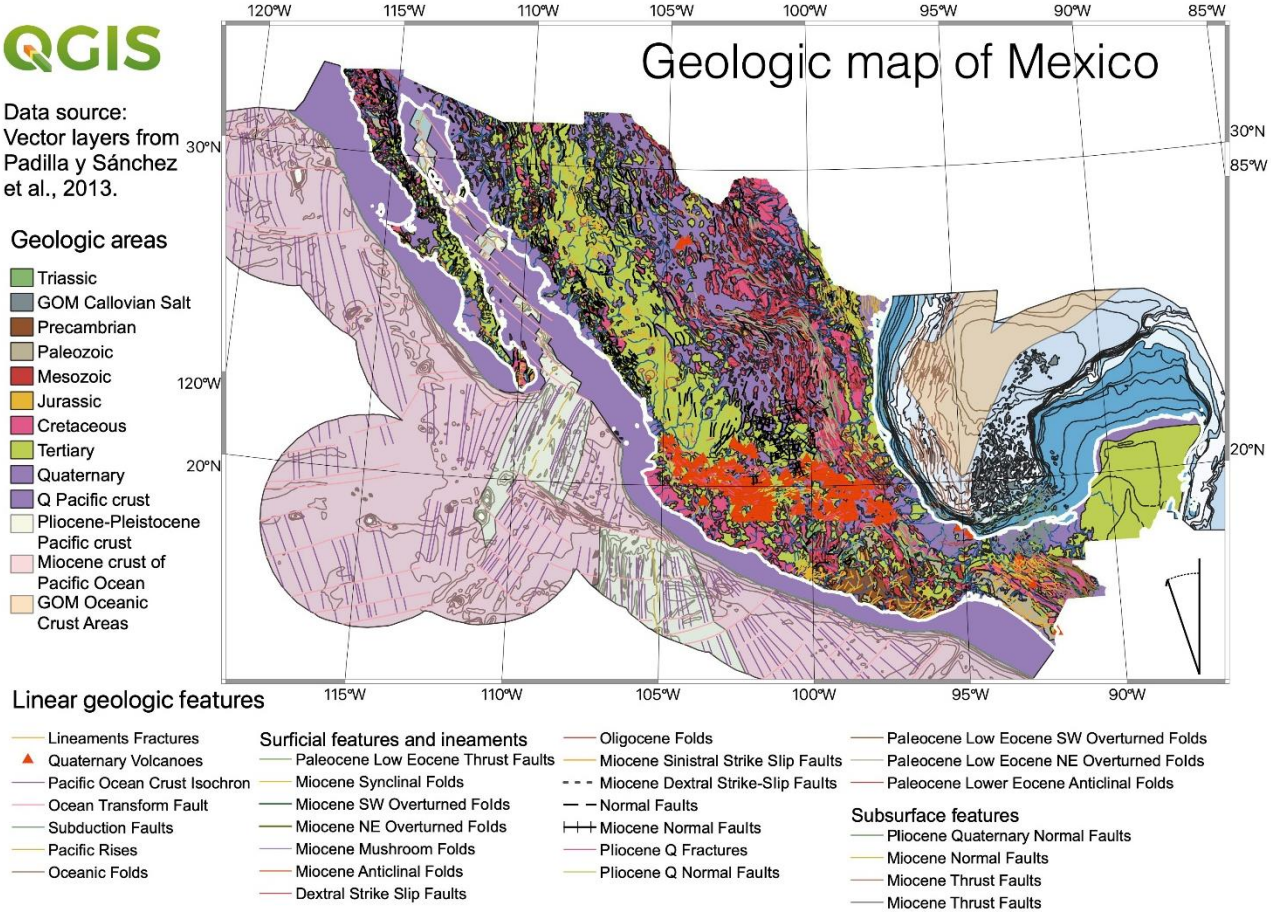

Source: Prepared by the author (2021). **Fonte:** Elaborado pelo autor (2021).

Such tectonic complexity and associated interrelated fault segments and lineaments create important regional potential seismic sources and favourable locations for possible earthquakes in Mexico (GÓMEZ-VASCONCELOS *et al.*, 2021; JIMÉNEZ, 2018). Therefore, due to the location in region of high tectonic activity briefly described above, Mexico is a country of special geologic vulnerability, exposed to seismic risks and prone to the repetitive earthquakes. For instance, recent Tehuantepec earthquake (Mw = 8.2, September 7, 2017) caused the following consequences:

> The [...] effects of the [...] Tehuantepec earthquake (Mw = 8.2), in cities and towns of the Mexican states of Chiapas and Oaxaca in a [...] 250 km from the epicenter [...] resulted in the death of 96 people and more than 110,000 houses damaged, where more than 41,000 were considered total losses (collapse, beyond repair or tagged for demolition (GODÍNEZ-DOMÍNGUEZ *et al.*, 2021, p. 1).

Another recent intense earthquakes in Mexico (September 19, 2017), with high magnitude (8.2 Mw) caused significant damages in housing which especially affected the soft-story buildings that are subject to strong motions (JARA *et al.*, 2020). It caused damage of 600 buildings and more than 1000 buildings classified in different risk levels. Losses and damages of engineering geological hazards, as well as their social and commercial consequences, are widely discussed in the existing literature (TENA-COLUNGA, 2021; SANTOS-REYES; GOUZEVA, 2020; MONTGOMERY *et al.*, 2020; LEMENKOV; LEMENKOVA, 2021a; MAYA-MONDRAGÓN *et al.*, 2019; ABELDAÑO ZUÑIGA *et al.*, 2019; LINDH; LEMENKOVA, 2021a, 2021b).

Active volcanism and faulting in the Trans-Mexican Volcanic Belt presents another consequence of tectonic and geologic processes in the region. The Trans-Mexican Volcanic Belt is a major volcanic arc which crosses Mexico from the Pacific Coast to the Gulf of México in an almost latitudinal direction and cause deformation events in the country (ALANÍZ-ÁLVAREZ; NIETO-SAMANIEGO, 2007). Furthermore, the geologic activity of the country is well expressed in its geomorphology which is expressed by the orogen as a continuation of the North American Cordilleran orogenic system. The Mexican orogen is extending for ca. 2000 km from NW–SE in general direction with local variations and having distinct spatial structure consisting of three parts:

> The Mexican orogen consists of (1) a western hinterland of accreted oceanic basinal rocks and magmatic arc rocks [...] the Guerrero volcanic superterrane, (2) a foreland orogenic wedge [...] the Mexican fold and thrust belt (MFTB), [...] Upper Jurassic-Lower Cretaceous carbonate rocks and Upper Cretaceous foreland-basin strata, and (3) [...] Late Cretaceous to Eocene foreland basins that lie northeast and east of the MFTB. The Mexican orogen encompasses the entire country, spanning several physiographic provinces (FITZ-DÍAZ *et al.*, 2018, p. 1).

Early geologic history of Mexico includes ‘11 deep orogenic systems composed altogether of more than 20 individual metamorphic complexes that span in age from the Paleoproterozoic (Statherian) to the middle Permian’ (ORTEGA-GUTIÉRREZ *et al.*, 2018; SPIKINGS *et al.*, 2015). More specifically, performed geologic investigations in Mexico revealed the following aspects in crustal evolution:

> Aspects for the tectonic history of the Earth, which includes the assembly and disruption of the three supercontinents [...] in Proterozoic-Paleozoic times. Major processes of modern plate tectonics that represent collisional, accretionary, and slab-related orogenic events involving continents and microcontinents, as well as island arcs and oceanic basins, marked the geologic architecture of the Mexican pre-Mesozoic basement (ORTEGA-GUTIÉRREZ *et al.*, 2018, p. 1).

Other evidence of the early geologic history in Mexican region dated Proterozoic to lower Palaeozoic time is exposed in southern Mexico (ÁNGELES-MORENO *et al.*, 2012) as a series of the metamorphic sequences providing an important geological record for Rodinia and NW Gondwana supercontinents, according to the performed modelling and simulating reconstructions (KEPPIE *et al.*, 2011).

As a result of the long Earth’s evolution in modern Mexico, orogen mountainous relief now extends over the major areas of the country which presents characteristic topographic features of elevated, active, continental margins formed as a result of the geologic history and tectonic activity (ALANIZ-ÁLVAREZ *et al.*, 1994). It is also reflected in patterns of the tectono-stratigraphic terranes and distribution of mineral resource over Mexico (CAMPA; CONEY, 1983), as well as regional volcanic stratigraphy of the Trans-Mexican Volcanic Belt which extends in central-southern Mexico (AGUIRRE-DÍAZ, 1996; FERRARI *et al.*, 2012).

The most notable geomorphological features of Mexico (**Figure 2**) include the following

mountain ranges: 1) Sierra Madre Oriental, which records the Jurassic opening of the Gulf of México and formation of the Late Cretaceous-Eocene Mexican Fold and Thrust Belt, which hosts large oil and gas reserves; 2) Sierra Madre Occidental, which continue the Rocky Mountains, has the oldest rocks in the country and one of the most active silicic volcanic provinces; 3) the Trans-Mexican Volcanic Belt (Sierra Nevada); 4) Sierra Madre del Sur, which records the formation and breakup of the supercontinents, the Rodinia and Pangea (MORA-KLEPEIS, 2021).

3. DATA AND METHODS

3.1. Data

We extracted topographic data from the General Bathymetric Chart of the Oceans (GEBCO) that covers both the terrestrial and the marine regions of the Earth with unprecedentedly high resolution of 15 arc second (SCHENKE, 2016; GEBCO COMPILATION GROUP, 2020). The reliability, quality and precision of GEBCO grid resulted in its applicability for topographic mapping as well reflected and discussed in cartographic works (HELFFRICH, 1996; CORTINA *et al.,* 2019; LEMENKOVA, 2020b, 2020c; MCMICHAEL-PHILLIPS, 2021). GEBCO dataset was successfully applied for cartographic modelling and visualization both on oceanic and terrestrial areas which is gained by smooth integration of the SRTM.

The seismic data showing earthquakes in Mexico from the monitor seismological stations for the period 2007-2021 has been used from the Incorporated Research Institutions for Seismology (IRIS) program (BUTLER *et al.,* 2004; ASTER *et al.,* 2005). The IRIS incorporates data from world seismic stations for geophysical monitoring and risk assessment (https://www.iris.edu/hq/). The IRIS provides a wide variety of seismic data from the thousands of seismic stations. These include time series data, continuous seismic recordings forming the archives of IRIS. Such archives include with metadata on seismograms including information on waveforms and events in a catalog. They also include source parameters from seismic catalogs and seismograms including old scanned images. This enables to get a higher-level view of the earthquakes and assess the seismicity. Thus, IRIS is a useful and reliable source of seismic information on earthquakes. The open source set of IRIS data include waveforms time, location with coordinates, depth, and magnitude of earthquakes. The IRIS data was used from the catalog and extracted as information for mapping **Figure 3**. The example of the information obtained from IRIS is presented in Table 1.

The Earth Magnetic Anomaly grid with 2-minute resolution was computed using NOAA dataset (MEYER *et al.,* 2017). The geophysical grids on gravity data for Mexico were extracted from the repositories of the UC San Diego, Scripps Institution of Oceanography (SIO), U.S. that includes the free-air gravity and vertical gravity grids with 1-arc minute resolution based on the remote sensing observations of the CryoSat and Jason-1 satellite missions (SANDWELL *et al.,* 2014). The geoid model was plotted based on the Earth Gravitational Model EGM-2008 with resolution of 2.5 arc minutes (PAVLIS *et al.,* 2012).

3.2. Methods

Main software tool used in present study for implementation of mapping is the Generic Mapping Tools (GMT) version 6.1.1, the advanced cartographic toolset that operates mapping from the console-based command line (WESSEL *et al.,* 2019). Visualizing of spatial distribution of earthquake events, topographic and geophysical data for Mexico was performed combining and adjusting GMT-based scripting techniques (GAUGER, 2007; LEMENKOVA, 2019b, 2019c).

In contrast to the traditional GIS used in mapping (CASTILLO-RODRÍGUEZ et al. 2010; GARCÍA-SORIANO *et al.,* 2020; MOREHART, 2012; KLAUČO *et al.,* 2013, 2017; LOZANO-GARCÍA *et al.*, 2020), the GMT is based on the scripting approach, that is, preparing map using bash

script (for instance, using the Xcode or Atom environments) that can be run from a GMT console, which is a terminal emulator, that is, a text-only computer interface.

Cartographic visualization controls the way spatial data are presented, and the colour palettes can correctly represent and highlight the correlations between the variables and geophysical phenomena. Therefore, colour tables were carefully selected for mapping in this study. The graphical colour palette for **Figure 2** has been adopted from existing works (THYNG *et al.*, 2016), and other have been used from the predefined colour tables of GMT: 'jet', 'wysiwyg', 'haxby', and 'hsv' by h5utils package of S.G. Johnson (https://github.com/NanoComp/h5utils).

Figure 2: Topographic map of Mexico. Mapping: Generic Mapping Tools

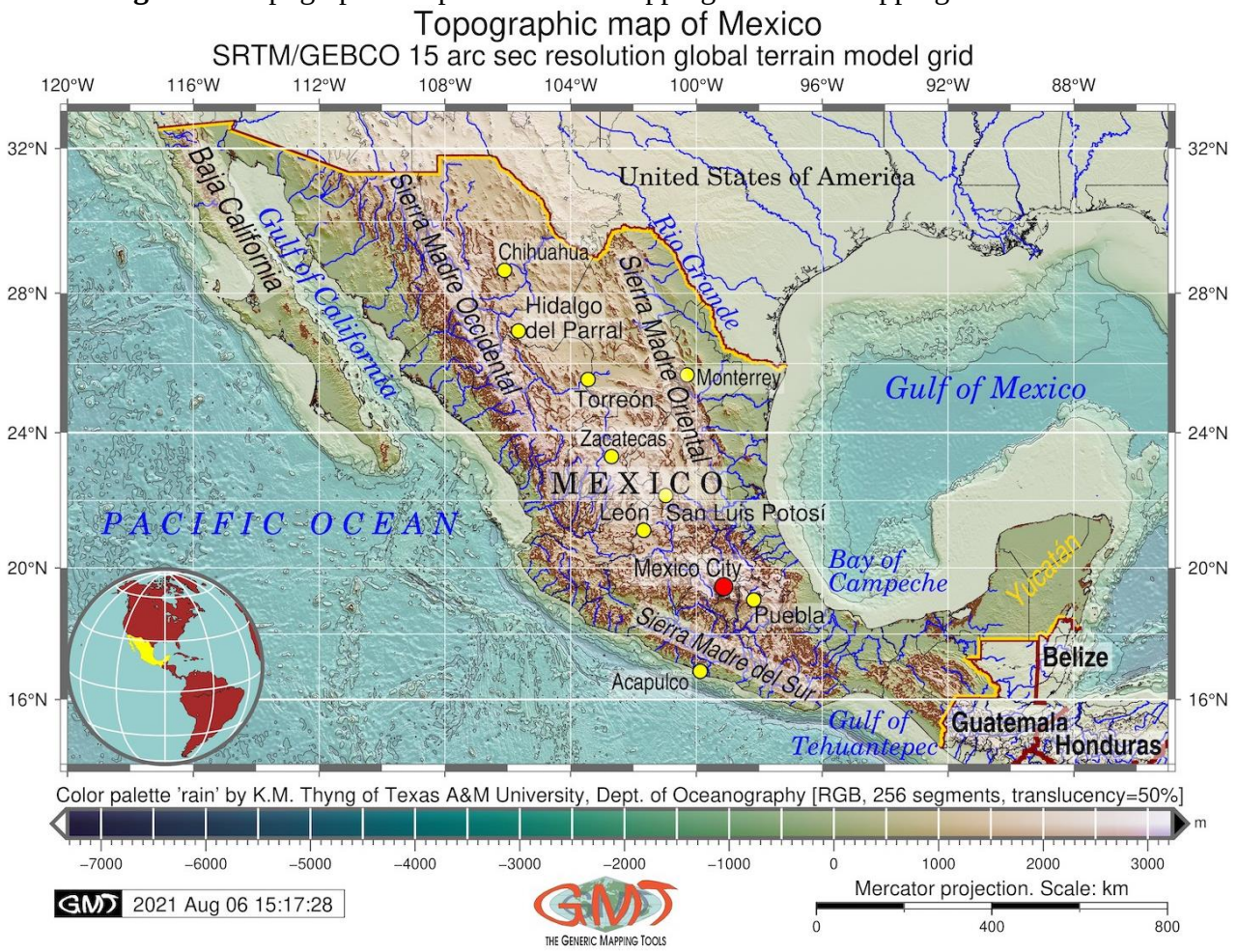

Source: Prepared by the author (2021). **Fonte:** Elaborado pelo autor (2021).

The technical examples of the GMT code are presented below for reference with the most essential snippets of the GMT script (here codes are shown for **Figure 2**):

- Mapping topographic map in **Figure 2** (visualization of GEBCO): "gmt grdimage mx_relief.nc -Cpauline.cpt -R240/275/14/33 -JM6i -P -I+a15+ne0.75 -t50 -Xc -K > $ps"
- Mapping seismicity in **Figure 3:** "gmt psxy -R -J quakes_MX.ngdc -Wfaint -i4,3,6,6s0.05 -h3 -Scc -Csteps.cpt -O -K >> $ps"
- Mapping magnetic anomalies in **Figure 4:** "gmt grdcut EMAG2_V2.grd -R240/275/14/33 -Gmx_mag.nc" and GDAL "gdalinfo mx_mag.nc -stats" for obtaining statistics.
- Mapping geoid in **Figure 5:** converting grid to the GMT format: "gmt grdconvert n00w90/w001001.adf geoid_02.grd" followed by the visualization: "gmt grdimage geoid_02.grd -Ccolors.cpt -R240/275/14/33 -JM6.5i -P -Xc -I+a15+ne0.75 -K > $ps"

- Mapping free-air gravity in **Figure 6** (here generating isolines): "gmt grdcontour grav_MX.grd -R -J -C100 -A200 -Wthinner -O -K >> $ps" for plotting lines by 100 mGal.

Mapping vertical gravity gradient in **Figure 7** (here converting the IMG to GRD format): "gmt img2grd curv_27.1.img -R240/275/14/33 -Ggrav_MX_v.grd -T1 -I1 -E -S0.1 -V". In total over 20 various GMT modules have been used using the demonstrated principle of console-based coding for cartographic visualization. This results in significant automatization of the scripts and their re-use for similar machine-based mapping purposes via the GitHub.

4. RESULTS

4.1. GEBCO-based topographic mapping of Mexico

The importance of using topographic information within the context of this work is explained by the need to analyse terrain elevation for evaluating the effects of regional variations in heights on seismicity pattern (mountainous regions or coastal areas). Specific problem that are assessed using topographic maps include regional and local aspects of seismic variability in geological setting, geomorphology and geoid heights as variables for integrated mapping. Therefore, plotting topographic map aims to demonstrate the variability of terrain in Mexico for data comparison with geology and seismicity using advanced cartographic technologies of GMT.

Topographic map of Mexico with surrounding coastal areas is shown on **Figure 2**. From GDAL inspection of the GEBCO dataset the following terrain range has been estimated for the topography of Mexico: Minimum=-7321, Maximum=3,235, Mean=-4267, StdDev=1333. The topography is varied and includes a range of landscapes such as coastal lowlands and plains, highlands, and mountain ranges in the Sierra Madre Oriental, Sierra Madre Occidental, Trans-Mexican Volcanic Belt (Sierra Nevada) and Sierra Madre del Sur, as shown in **Figure 2**. The topographic variability of Mexico creates favourable conditions for different climate zones varying across the country accordingly. Besides, Mexico is notable for unique geomorphological landforms.

4.2. Quantitative analysis of seismicity in Mexico

The importance of using seismological data in the context of the present work consists in the novel insights that IRIS brings into seismic analysis. Integrated analysis of earthquakes compared with topography and tectonic setting of the country reveals correlations of the seismically active zones with subduction of the tectonic plates. Moreover, seismicity reflects geologic processes and tectonic settings of the country, which is visible using comparative analysis of maps presented by the advanced cartographic tools. Therefore, the presented maps are useful for seismologists. The use of GMT in seismology reflects the development of data size from medium-scale to big data because seismic data are collected continuously. Big data cannot be processed manually and requires scripting methods of GMT. The balance here is between rapidly developed cartographic methods and the increasing amount of seismic data provided by IRIS.

The most significant earthquakes in Mexico (**Figure 3**) are located in the Trans-Mexican Volcanic Belt in south-central Mexico, where a series of earthquakes with magnitude from 1.5 to 7.2 are analysed based on the IRIS database system for the period of 2007 to 2021. The earthquake with the lowest magnitude of 1.5 was detected 12 km S of Smiley, Texas on depth 10 km. Based on the spatial analysis and correlation of earthquake distribution with geologic, geophysical and topographic setting of Mexico, following major sources of earthquakes have been identified:

i) earthquakes located along the Middle American Trench marking the subducting zone of the Cocos Plate under the North American Plate;

ii) a notable belt of earthquakes located along the active Trans-Mexican Volcanic Belt;

iii) earthquakes situated along the borders of the subducting tectonic plates – Cocos, Orozco and Rivera plates;

iv) earthquakes situated in the Gulf of California marking the tectonic fracture zones.

Figure 3: Seismicity map of Mexico. Mapping: Generic Mapping Tools

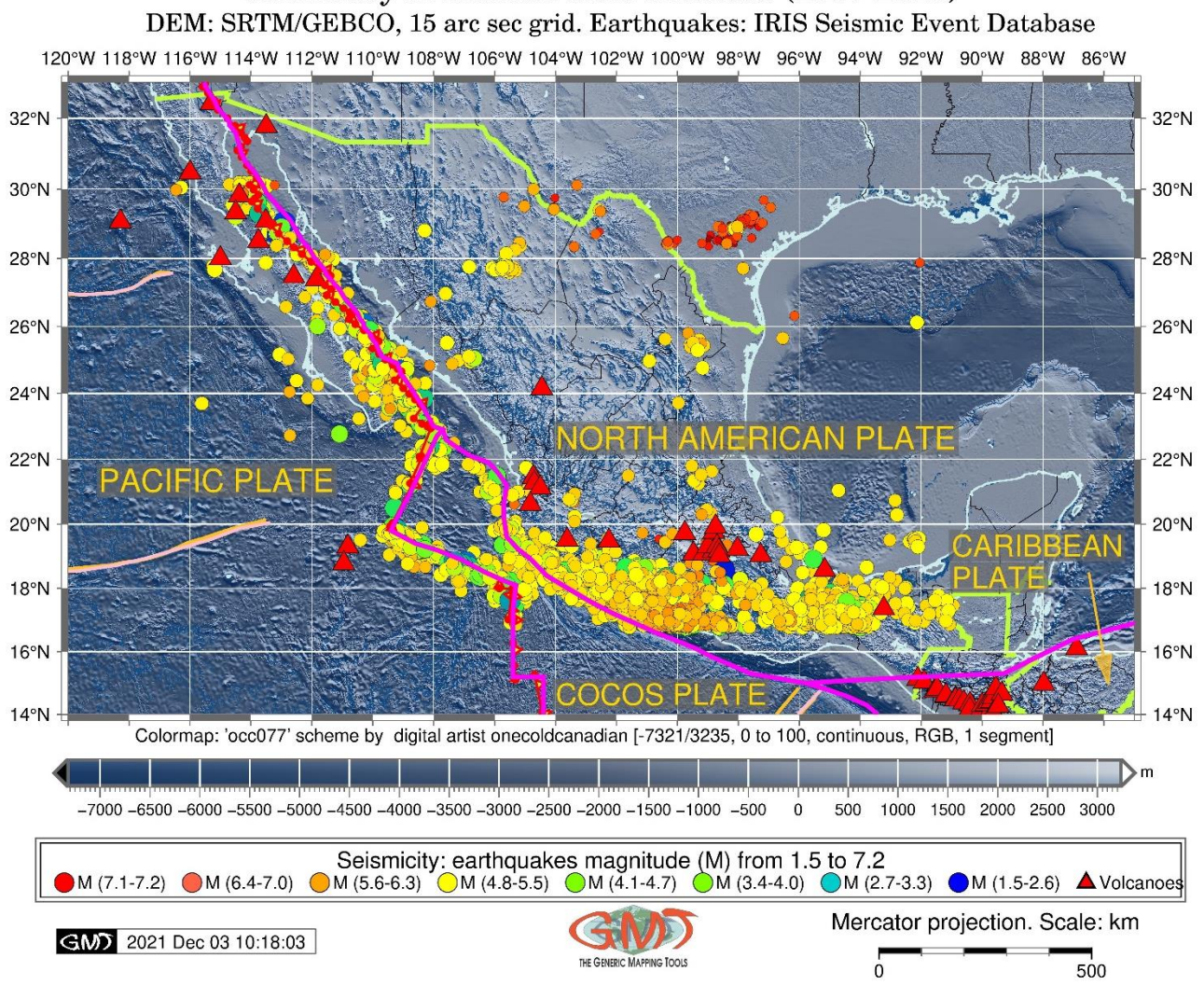

Source: Prepared by the author (2021). **Fonte:** Elaborado pelo autor (2021).

Other notable seismic active areas are visible along the tectonic plate borders, especially those separating the Rivera Plate from the Pacific Plate with almost rectangular borders (**Figure 3**) generated by tectonic activity and slab movements. Comparison of the location of seismic events with active volcanic chain of the Trans-Mexican Volcanic Belt shows that vulnerable and prone to earthquakes regions in Mexico are located near volcanic active zones with complex geology.

Table 1: Earthquakes in Mexico with the highest magnitude (>6.0) according to IRIS (2007-2021)

Date (yyyymmdd)	Time (UTC)	Lat (N)	Lon (W)	Depth	Mag (Mw)	Region in Mexico
20140418	14:27:24	17°23'49"	100°58'20"	24	7.2	33km ESE of Petatlan
20170919	18:14:38	18°32'60"	98°29'19"	48	7.1	1km E of Ayutla
20120412	07:15:48	28°41'45"	113°6'14"	13	7	Baja California
20090803	17:59:56	29°2'20"	112°54' 11"	10	6.9	Sonora
20150913	08:14:08	24°54'46"	109°37'22"	10	6.7	95km SW of Topolobampo
20101021	17:53:13	24°41'45"	109°9'22"	13	6.7	Gulf of California

Date (yyyymmdd)	Time (UTC)	Lat (N)	Lon (W)	Depth	Mag (Mw)	Region in Mexico
20160121	18:06:57	18°49'26"	106°56'1"	10	6.6	215km SW of Tomatlan
20131019	17:54:54	26°5'28.6"	110°19'15"	9.5	6.6	99km SW of Etchoropo
20110407	13:11:22	17°12'29"	94°20'16"	166.2	6.6	Veracruz
20120411	22:55:10	18°13'44"	102°41'20"	20	6.5	Michoacan
20111211	01:47:25	17°59'10"	99°47'20"	59	6.5	Guerrero
20140508	17:00:14	17°14'6"	100°44'46"	17.1	6.4	6km WSW of Tecpan de Galeana
20090924	07:16:20	18°49'44"	107°20'20"	13	6.4	off the coast of Jalisco
20080924	02:33:05	17°36'43"	105°29'49"	12	6.4	off the coast of Colima
20180119	16:17:44	26°41'10"	111°4'42.6"	10	6.3	78km NNE of Loreto
20160607	10:51:37	18°21'49"	105°10'23"	10	6.3	106km SSW of San Patricio
20140729	10:46:14	17°40'54"	95°39'12"	107	6.3	24km SE of Playa Vicente
20120925	23:45:24	24°39'58"	110°10'23"	10	6.3	Baja California Sur
20111101	12:32:00	19°49'52"	109°12'18"	10	6.3	Revilla Gigedo Islands
20150222	14:23:12	18°40'36"	106°50'53"	5	6.2	218km SW of Tomatlan
20140906	19:22:59	18°45'10"	-107.0488	17	6.2	229km SW of Tomatlan
20140531	11:53:46	18°47'15"	107°2'56"	5	6.2	265km WSW of Tomatlan
20130821	12:38:29	16°52'42"	99°29'53"	21	6.2	18km WNW of San Marcos
20100824	02:11:59	18°47'42"	107°11'35"	10	6.2	off the coast of Jalisco
20090803	18:40:50	29°18'36"	113°43'41"	10	6.2	Baja California
20200522	08:46:06	22°24'54"	108°7'39"	10	6.1	176km ESE of San Jose del Cabo
20141008	02:40:53	23°50'39"	108°19'52"	10	6.1	111km WSW of El Dorado
20121115	09:20:21	18°20'46"	100°22'55"	53	6.1	Guerrero
20070901	19:14:22	24°54'7"	109°41'20"	9	6.1	Gulf of California
20140510	07:36:01	17°13'9"	100°48'44"	23	6	14km WSW of Tecpan de Galeana
20130422	01:16:32	18°4'52"	102°10'55"	30	6	20km NNW of La Union
20120412	07:06:00	28°50'13"	113°1'37"	9	6	Baja California
20110726	17:44:20	25°6' 4"	109°31'30"	12	6	Gulf of California
20090703	11:00:14	25°7'52"	109°45'14"	10	6	Gulf of California

Source: IRIS (2021). **Fonte:** IRIS (2021).

4.3. Geoid fields

The geoid shows a model of global mean sea level used to evaluate precisely terrain heights. Variations of the geoid show different gravity fields that well reflect geophysical setting of the Earth. In this study the geoid raster grid is based on the National geopotential model of the Earth's gravity fields (EGM-2008) selected and clipped for the region of Mexico. The EGM-2008 is set up as a 2.5-minute grid of xyz values in the tide-free system (PAVLIS *et al.*, 2012).

This is an updated and improved version of the initial geoid global grid of EGM96 Geopotential Model which had a 15-minute resolution. The geoid undulations corresponds to the ideal mean-earth ellipsoid model of the Earth with undulations referenced to the World Geodetic System 1984 (WGS 84). The correlation between the WGS 84 and gravity in the geoid consists in the numeric constant parameters used to model reference ellipsoid of the Earth (HOFMANN-WELLENHOF *et al.*, 1993) and gravity models. Quantitative interpretation of the geophysical field anomalies in geoid (**Figure 4**) has been performed using GDAL library embedded in GMT.

The extreme values of the geoid undulations are associated with the anomalous gravity values that change due to the land mass deficit, since the Earth's mass is generally unevenly distributed. The generalized isolines of geoid (in meters) are plotted and modelled on the basis of the EMG2008 with interval of 1 m (**Figure 4**). The general increase of the geoid values is notable from NW (Pacific Ocean, dark blue colours in **Figure 4**, minimal value = -47 m) in SE direction towards Guatemala and southern Mexico: maximal value=10 m, bright red colours in **Figure 4**. In terms of geological interpretation, this means that the gravity values are higher in the southern Mexico. That is, higher values of geoid indicate on stronger gravity field as a result of the mountainous region on

the south of the country. In contrast, the geoid heights are lower in the regions of the deep ocean (the lowest values that correspond to the dark blue colour in **Figure 4**) and in the lowlands (light green to aquamarine colours in **Figure 4**). The geoid shows higher values in the mountain regions because mountains have more mass than lowlands, valleys or oceanic crust, Therefore, the pull of gravity is regionally stronger near mountains which can be seen in **Figure 4**.

Figure 4: Geoid model of Mexico. Mapping: Generic Mapping Tools

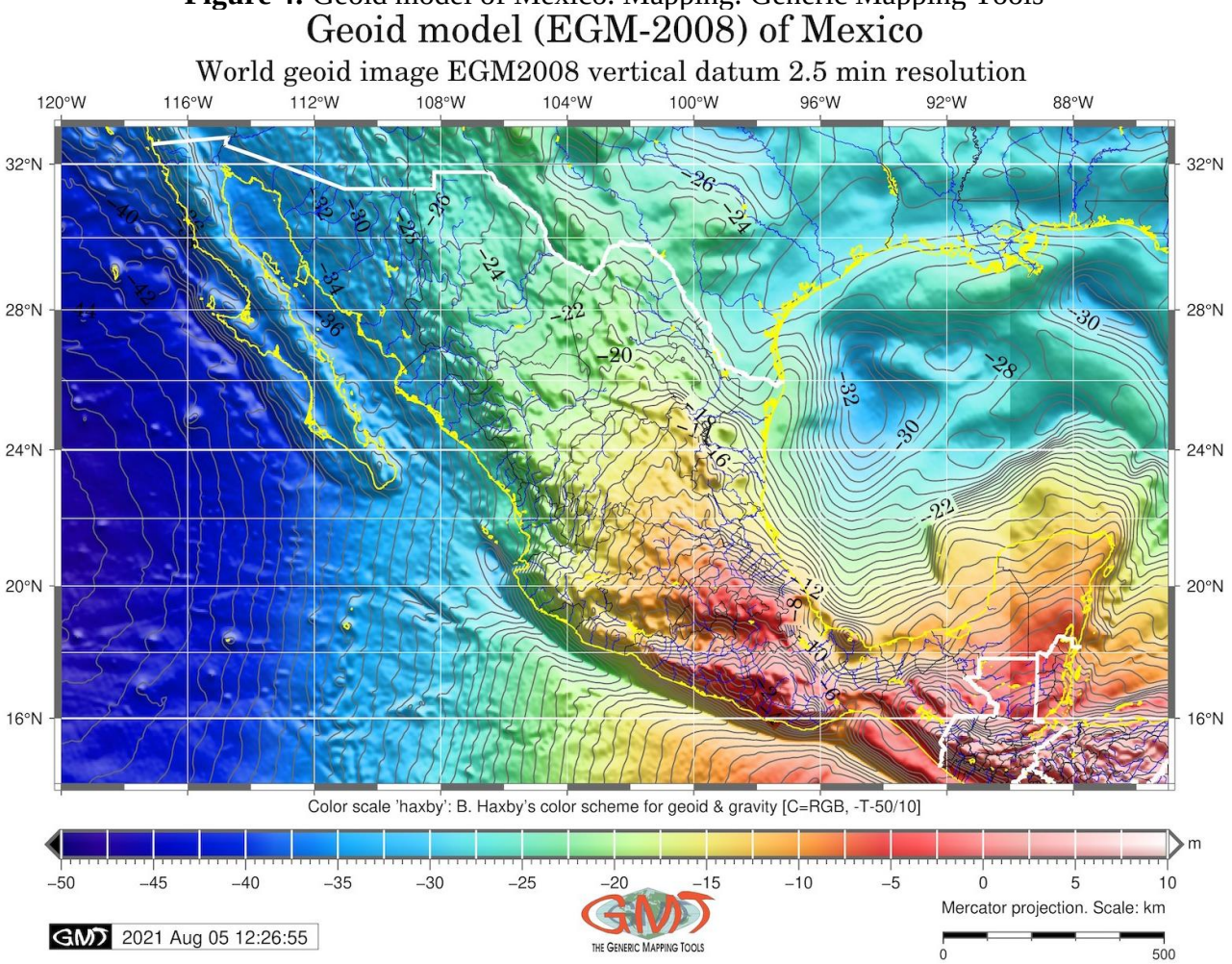

Source: Prepared by the author (2021). **Fonte:** Elaborado pelo autor (2021).

4.4. Magnetic anomalous fields

The importance of mapping the magnetic anomalous fields in the content of this research consists in linking the geology and tectonics of Mexico and surrounding oceanic region. Complex geologic past of Mexico involved processes of formation of the oceanic crust in the coasts of the Pacific Ocean that in turn reflected in current seismicity of the subduction zone. Namely, the source of the magnetic anomalies is magnetization carried by titanomagnetite minerals in igneous rocks, such as basalt and gabbros. These minerals are magnetized during formation of the ocean crust at the ocean ridges in the geological past. Along with upward rising and cooling of magma on the surface, the rock gets magnetization directed of the field of movement of magma. The distribution of the magnetic anomalies visualized on the map (**Figure 5**) can be used for the analysis of these geologic processes in the past.

The magnetic data (**Figure 5**) were applied from the Earth Magnetic Anomaly Grid with 2-arc minute resolution, (EMAG2) in GMT Grid format from the NOAA repository (MAUS *et al.*,

2009; EMAG2, 2009). The EMAG2 project integrates all satellite, ship, and airborne magnetic measurements for a dataset with global coverage thus presenting a big data approach in geophysical mapping (**Figure 5**).

Figure 5: Magnetic anomaly grid for Mexico. Mapping: Generic Mapping Tools

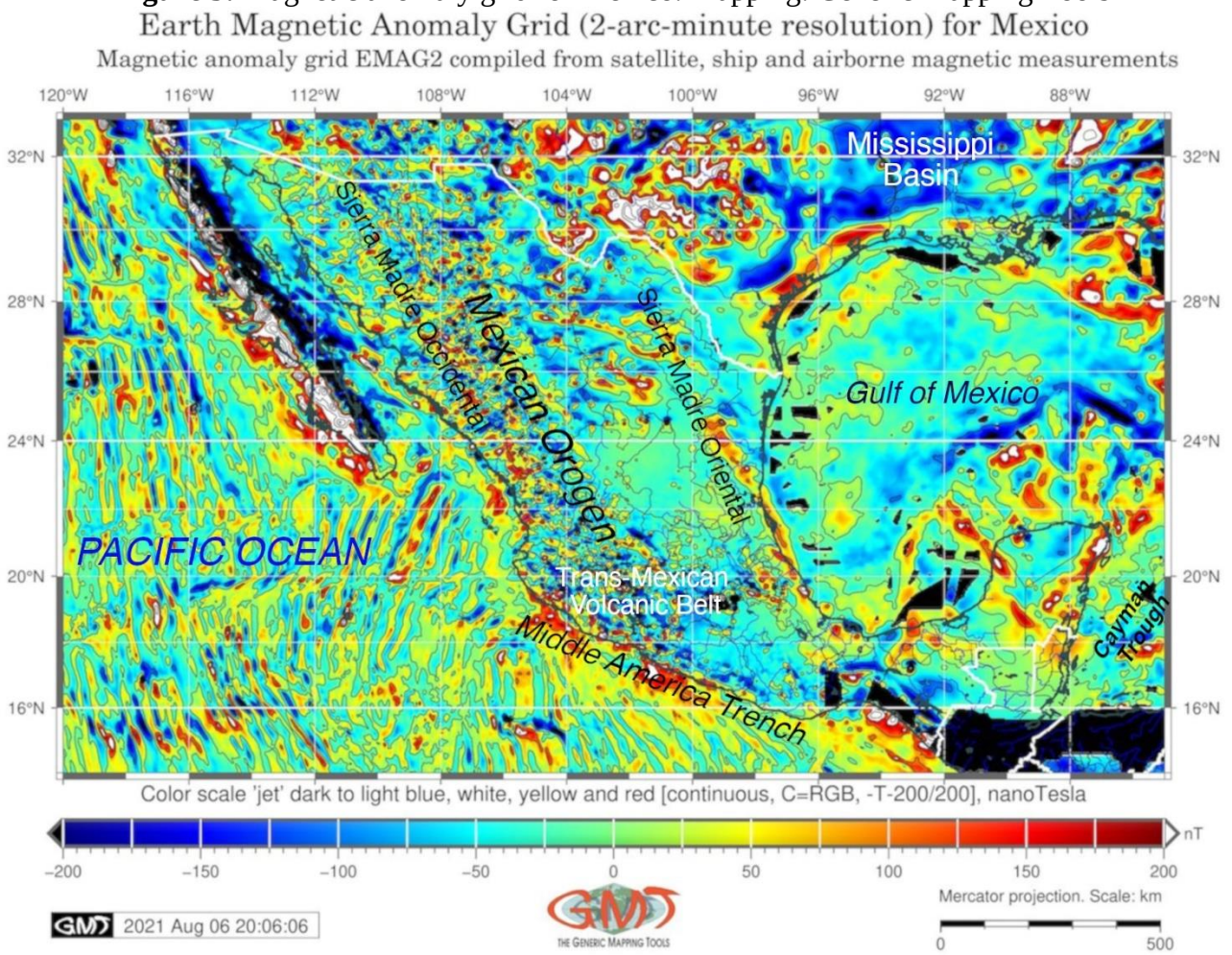

Source: Prepared by the author (2021). **Fonte:** Elaborado pelo autor (2021).

The mapped magnetic anomaly over Mexico (**Figure 5**) has been compared with the geoid and topographic maps (**Figures 1 and 3**) to find regional correlations between the data. A visual analysis indicates the negative magnetic values (between -100 to -200 nanoTesla) in the region of Mississippi river (dark blue colours in **Figure 5**), while the complex topography of Mexico within orogenic belts of Sierra Madre Oriental and Sierra Madre Occidental in the central part of the country mostly have positive values (yellow to red colours in **Figure 5** that correspond to values 50 to 200 nanoTesla). The Trans-Mexican Volcanic Belt (Sierra Nevada) are marked with moderate magnetic anomalies (values of -50 to 10 nT, cyan to aquamarine colours in **Figure 5**).

The cartographic visualization of EMAG2 in **Figure 5** shows a complex mosaic variation in the magnetic anomaly values over Mexico with certain homogeneous areas in central Mexico and highly heterogeneous pattern of magnetic anomalies over the Pacific Ocean seafloor and in the mountainous regions of the orogenic belts of Mexico and the Trans-Mexican Volcanic Belt (Sierra Nevada), **Figure 5**. A certain correlation exists between the magnetic field map based on EMAG2 in **Figure 5**, the topographic map in **Figure 2** and free-air gravity map showing geophysical variations in **Figure 6**, which proves the effects of the geophysical setting on the topographic relief and geomorphological landforms in Mexico. The correlation between topography, magnetic anomaly, and gravimetric anomaly found in the distribution of values as indicated on the variations of fields. Thus

it shows the degree to which the geophysical variables change in values in accordance with one another and to the topographic and geologic data.

4.5. Free-air gravity anomalous grids

The map of free-air gravity anomaly of Mexico shows measured gravity anomaly in Faye's reduction after the correction on the elevation heights in the point of measurements. In geophysics, the altimetry corrections for gravity data include the information on derived from topographic data. This map shows the gravitational effect of the topography above mean sea level near the measurement point. The reduction of Faye does corrections by adjusting measurements of gravity to those that could have been measured at a reference level, that is, mean sea level or the geoid.

Figure 6: Free-air gravity anomaly map. Mapping: Generic Mapping Tools

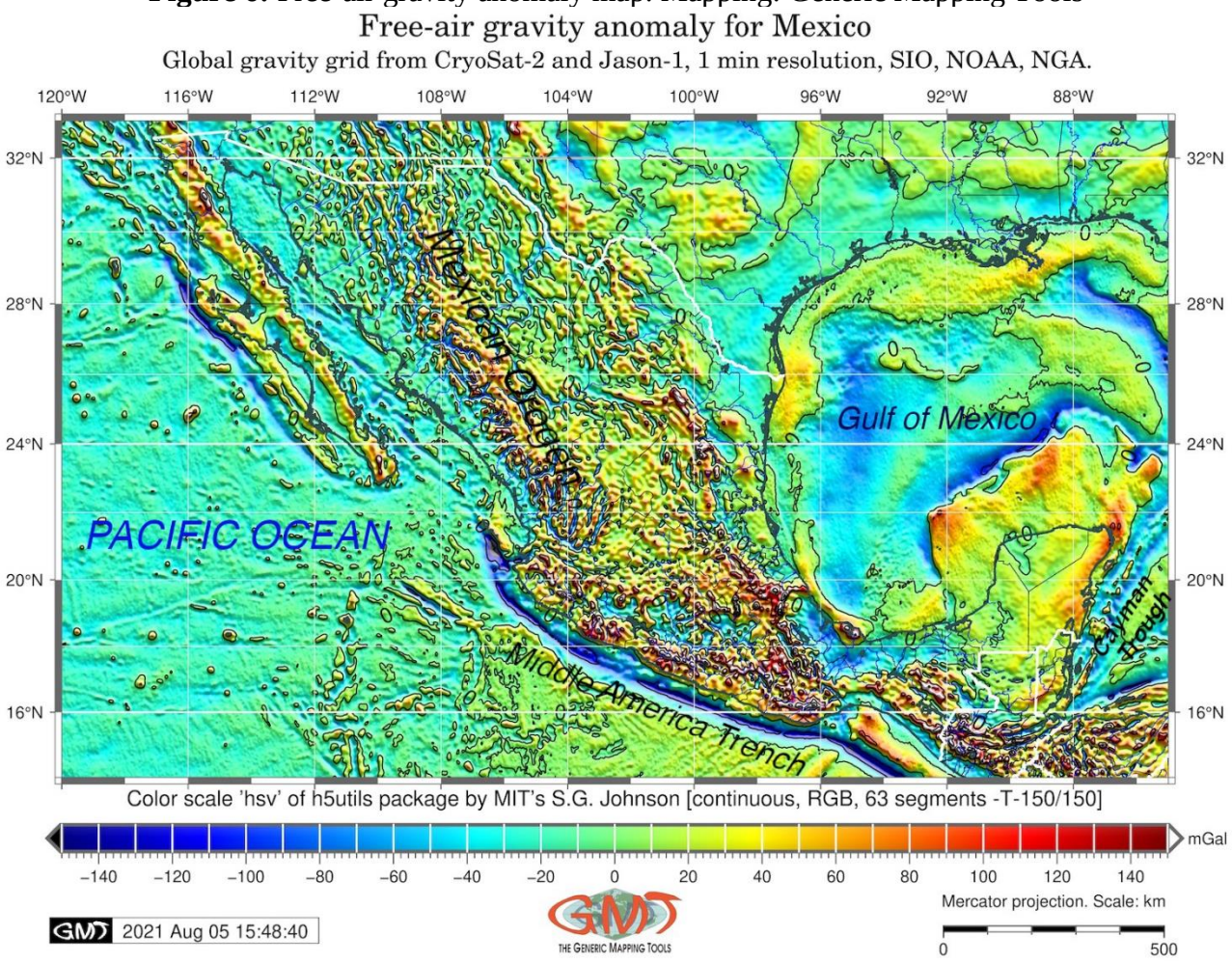

Source: Prepared by the author (2021). **Fonte:** Elaborado pelo autor (2021).

The map showing free-air gravity anomaly in mGal (**Figure 6**) demonstrates a well correspondence with regional topography and geoid variations over Mexico. Specifically, the varied pattern the geophysical isolines presented over the Mexican orogen (**Figure 6**) well correlates with the geomorphology of the country showing higher values (120 up to 150 mGal) in the mountains. On the contrary, lower values of gravity (**Figure 6**) can be noted over the deepest seafloor areas in the Middle American Trench and the Cayman Trough in the Caribbean Sea (blue areas with values of gravity below -140 mGal in **Figure 6**). The most of the seafloor over the Pacific Ocean corresponds to the values -40 to -20 (cyan colours in **Figure 6**), that is, moderate to low values. It is worth noting that the topography of the Baja California and the adjacent Gulf of California are particularly well

correlating with GEBCO grid. Hence, the relief of the country can be well followed using the comparison of the topographic and geophysical patterns over Mexico.

4.6. Vertical gravity gradient

Vertical gravity anomaly is the computed normal gradient of gravity showing variations in gravity along with change of heights in free air (**Figure 7**). It shows the difference between the actual and normal gravity at the same point. Thus, the correspondence between vertical gradient of gravity anomaly and curvature of geoid consists in the discrepancy between the mean curvatures of geoid and quasi-geoid. Vertical correction of the gravity shows a high-pass filtered version of gravity that normally presents more detailed fluctuations in data.

Figure 7: Vertical gravity gradient for Mexico. Mapping: Generic Mapping Tools

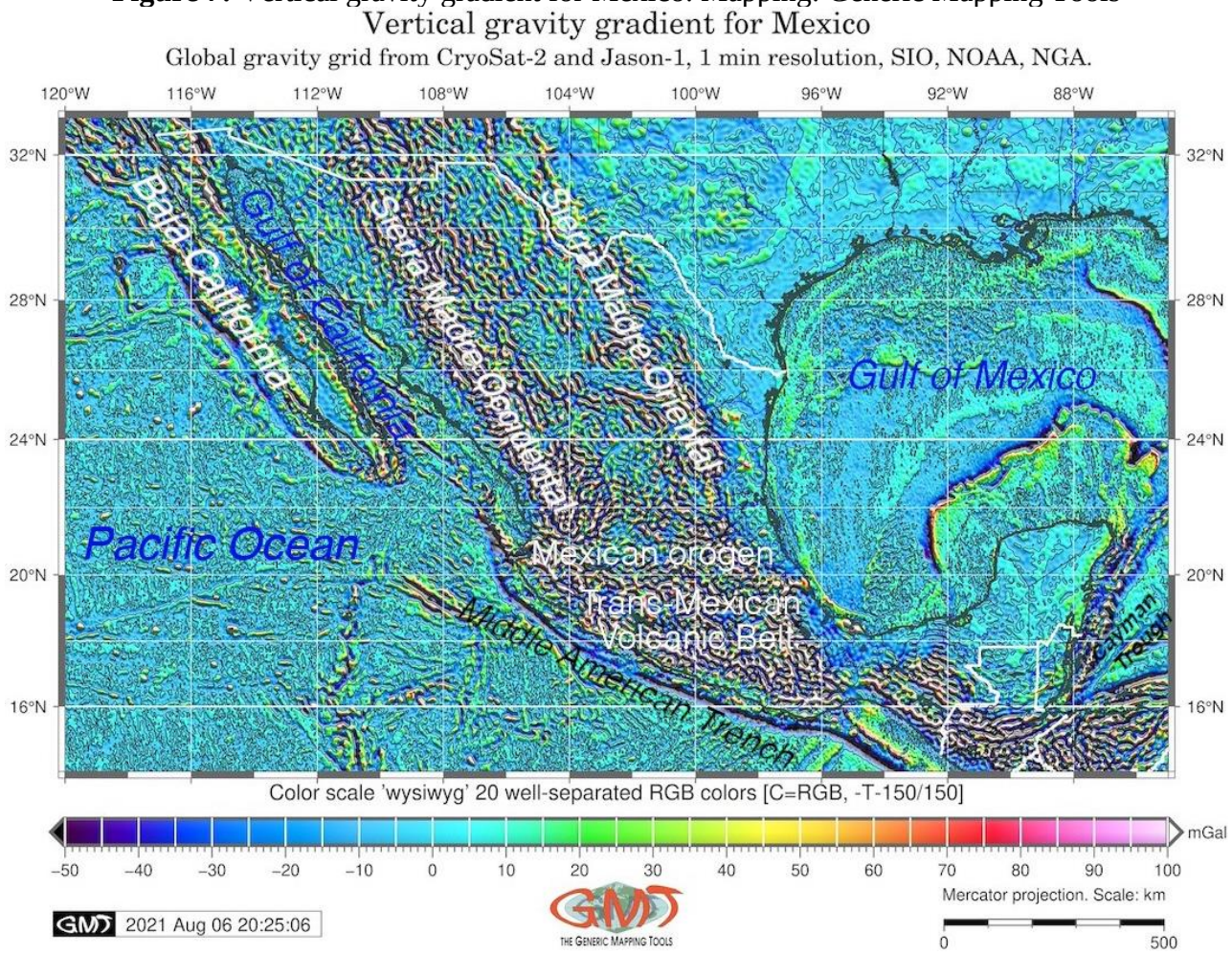

Source: Prepared by the author (2021). **Fonte:** Elaborado pelo autor (2021).

The obtained vertical gravitational gradient is based on the satellite derived gravity computations and showed the characteristics of gradient (i.e. changes and variations in values) as computed using methods developed to examine vector and variability in geophysical anomalies. As can be noted (**Figure 7**) in general, the analysis of the vertical gradient grid indicates a significant difference in gravity values in the Mexican orogen while more homogeneous values (blue to cyan colours in **Figure 7** which corresponds to the values of ca. -10 to 10).

The comparison of data covering regions of the Pacific oceanic seafloor and the Caribbean Sea with terrestrial areas of Sierra Madre Occidental and Sierra Madre Oriental as well as the Trans-Mexican Volcanic Belt shows the significant difference and well correlates with the **Figure 6** of free-

air gravity of Mexico. The lowest values (dark blue colours in **Figure 7**) are dominating mostly over the deep-sea trenches – the Middle American Trench and the Cayman Trough, as well as the Gulf of California where the gravity anomalies change rapidly comparing with the adjacent terrestrial regions.

5. DISCUSSION

In this study we aimed at geospatial data handling for mapping geological and geophysical setting of Mexico using information derived from the open source data. This study includes an interdisciplinary context by linking the open geospatial data from a number of disciplines and science clusters. Specifically, we used data and methods from several domains and disciplines: 1) computer science (algorithms of GMT bash scripting for data processing from the console); 2) geospatial engineering (processing of raster, vector and tabular data in various formats), 3) cartography and GIS (mapping, design and visualization); 4) geology, environment and Earth (analysis and interpretation of several geological and geophysical datasets using new seven maps); 5) seismicity of Central America with a case of Mexico (mapped earthquakes with magnitudes and locations); 6) applied geophysics and geology (data analysis using modelling of magnetic anomalies and geophysical anomaly grids).

There are examples of similar integrated complex studies that include a multi-disciplinary approach combining morphologic, stratigraphic, sedimentary, petrographic, geologic and geochemical data for mapping and analyses of the correlations among the phenomena and geodynamical processes of the Earth (e.g. GUILBAUD *et al.*, 2021; GRAHAM *et al.*, 2020; GOHL *et al.*, 2006; GÓMEZ-TUENA *et al.*, 2018; SUETOVA *et al.*, 2005a; VÁZQUEZ *et al.*, 2021).

Gravity, geoid and magnetic data of the Earth present one of most powerful tools for regional geophysical, geological and seismic studies of both lithosphere and mantle of the Earth. Integration of such data for a project aimed at complex mapping of the seismically active zone aims to explore seismic risks and possibility of earthquake distribution over Mexico. The integration of such multi-source data enables to perform the long-term seismological prognosis and evaluation of risks in the southern Mexico around the Trans-Mexican Volcanic Belt through analysis of the correlation between the topographic and geophysical data.

Besides, GMT-based mapping using geophysical, topographic and seismic data combination assists in developing strategy for mineral exploration in selected regions of Mexico, and assists in modelling strategic oil and gas wells and basins. Important hydrocarbon resources of Mexico are located along the coasts of the Gulf of Mexico, several basins (Pedregosa, Sabinas, Parras, Burgos) are located in the NE of the country, significant oil and gas reserves are situated in the Gulf of California. Exploration of such rich resources, development, prognosis and risk assessment while maintaining shelf exploration require detailed and accurate mapping and analysis of potential risks in seismically active country such as Mexico.

Therefore, modelling geologic, seismic and geophysical data using integrated GMT-based mapping by machine learning scripting methods enables to get better insights into the correlations between the tectonic and geophysical phenomena and processes and enable to perform modelling and prognosis tasks and seismic risk assessment.

6. CONCLUSION

The advantages of the demonstrated GMT-based mapping consists in the high level of the machine graphics that enables to produce print-quality maps with minimized human routine in the workflow. Therefore, the application of GMT scripting and machine learning in cartography makes cartographic plots visually appealing which can highlight correlations between the geophysical phenomena. Moreover, variations in depicted gravity and magnetic fields encourage further analysis of the visualised phenomena and their comparison with topographic settings of Mexico.

The study presented following major outcomes:

- application of the advanced cartographic scripting by GMT for integrated analysis of the multi-source high-resolution data covering Mexico: topographic GEBCO grid, geophysical data that include magnetic EMAG raster, geoid EMG-2008, satellite derived gravity grids, seismological IRIS based data for 2007-2021 with data on focal depth, magnitude, time and location of earthquakes in Mexico.
- application of the remote sensing based satellite-derived gravity data based on the missions of the CryoSat-2 and Jason-1 helps detect tectonic structure in the terrestrial topography of Mexico and oceanic seafloor of the Gulf of Mexico and the coastal regions of the Pacific Ocean (e.g. rectangular contours of the Rivera and Orozco tectonic plate). Moreover, the presented series of the thematic maps plotted in identical cartographic projections enabled to perform comparative analysis for detecting geophysical and geodynamic setting of Mexico.
- finding and highlighting correlations between the geophysical data (gravity, geoid, magnetism) and regional tectonic and geodynamic variations that correspond to the topographic relief over the territory of Mexico based on the analysis of the six new maps.

GMT plots as graphic representations of the earthquakes and topographic and geophysical variations are conventionally constructed from the scripting approach using GMT console. In this study, we provide the GMT codes which were used to visualise the variables in geophysical input data using a modular method when every line of code represents the variable. This approach overcomes the time and labor-intensive disadvantages of the conventional mapping methods by GIS. In addition, the range of geospatial datasets for mapping has been used in this study from available open sources to visualize data controlled by geophysical and geological setting of Mexico. The cartographic scripting toolset GMT is open-source and available for download and use.

The principle, usage and application cases of the scripts are introduced in this paper with the examples of the cartographic workflow. The validity of the scripts and cartographic method for geophysical and geological investigations of Mexico is demonstrated using the series of maps plotted in identical map projection. Due to the need for geophysical exploration and seismic research, data of earthquakes and topography of Mexico have been collected and visualised in this article. The GMT approach together with available open geophysical data on Mexico, such as the magnetic anomalies or gravity anomalies, can use these data to make analysis of seismicity and earthquake predictions and correlations with regional topography more efficient, and thus improve and geophysical research and geological exploration in Central America.

ACKNOWLEDGEMENT

O autor agradece aos revisores e editores pela revisão e edição deste manuscrito.

REFERÊNCIAS

ABELDAÑO ZUÑIGA, R. A.; REYES, G. G.; SILICEO MURRIETA, J. I.; GONZÁLEZ VILLORIA, R. A. M. Posttraumatic stress symptoms in people exposed to the 2017 earthquakes in Mexico. **Psychiatry Research**, Oaxaca, v. 275, p. 326-331, May. 2019. DOI: https://doi.org/10.1016/j.psychres.2019.04.003.

AGUIRRE-DÍAZ, G. J. Volcanic stratigraphy of the Amealco caldera and vicinity, central Mexican Volcanic Belt. **Revista Mexicana de Ciencias Geológicas,** [S.L.], v. 13, n.1. p. 10-51, 1996.

AGUIRRE-DÍAZ, G. J.; LÓPEZ-MARTÍNEZ, M. Geologic evolution of the Donguinyó-Huichapan caldera complex, central Mexican Volcanic Belt, Mexico. **Journal of Volcanology and Geothermal Research**, [S.L.], v. 179, n. 1–2, p. 133-148, jan. 2009. DOI: https://doi.org/10.1016/j.jvolgeores.2008.10.013.

ALANIZ-ÁLVAREZ, S. A.; NIETO-SAMANIEGO, A. F.; ORTEGA-GUTIÉRREZ, F. Structural evolution of the Sierra de Juarez mylonitic complex, State of Oaxaca, Mexico. **Revista Mexicana de Ciencias Geológicas**, [S.L.], v. 11, n.2, p. 147–156, 1994.

ALANÍZ-ÁLVAREZ, S. A.; NIETO-SAMANIEGO, A. F. The Taxco–San Miguel de Allende fault system and the Trans-Mexican Volcanic Belt: two tectonic boundaries in central México active during the Cenozoic. In: ALANIZ ÁLVAREZ, S. A.; NIETO SAMANIEGO, A. F. (eds.). **Geology of México:** Celebrating the Centenary of the Geological Society of México, Geological Society of America Special Paper, [S.L.], v. 422, p. 301–316, jan. 2007.

ÁNGELES-MORENO, E., ELÍAS-HERRERA, M., MACÍAS-ROMO, C., SÁNCHEZ-ZAVALA, J.L. AND ORTEGA-GUTIÉRREZ, F. **Geological Map of the Western Border of Cuicateco Terrane, Southern Mexico**. Geological Society of America: Map & Chart Series MCH102, 2012. Available at: https://www.worldcat.org/title/geological-map-of-the-western-border-of-the-cuicateco-terrane-southern-mexico/oclc/781807626 Acesso em: 27 jan. 2022.

ARCE, J. L.; LAYER, P. W.; MACÍAS, J. L.; MORALES-CASIQUE, E.; GARCÍA-PALOMO, A.; JIMÉNEZ-DOMÍNGUEZ, F. J.; BENOWITZ, J.; VÁSQUEZ-SERRANO, A. Geology and stratigraphy of the Mexico Basin (Mexico City), central Trans-Mexican Volcanic Belt. **Journal of Maps**, [S.L.], v. 15, n. 2, p. 320-332, apr. 2019. DOI: https://doi.org/10.1080/17445647.2019.1593251.

ARCE, J. L.; FERRARI, L.; MORALES-CASIQUE, E.; VASQUEZ-SERRANO, A.; ARROYO, S. M.; LAYER, P. W.; BENOWITZ, J.; LÓPEZ-MARTÍNEZ, M. Early Miocene arc volcanism in the Mexico City Basin: Inception of the Trans-Mexican Volcanic Belt. **Journal of Volcanology and Geothermal Research**, [S.L.], v. 408, n. 107104, p. 1-18, dec. 2020. DOI: https://doi.org/10.1016/j.jvolgeores.2020.107104

ASTER, R.; BEAUDOIN, B.; HOLE, J.; FOUCH, M.; FOWLER, J.; JAMES, D. IRIS Seismology Program marks 20 years of discovery. **Eos, Transactions American Geophysical Union**, [S.L.], v. 86, n. 17, p. 171–172, apr. 2005. DOI: https://doi.org/10.1029/2005EO170002.

BLATTER, D. L.; HAMMERSLEY, L. Impact of the Orozco Fracture Zone on the central Mexican Volcanic Belt. **Journal of Volcanology and Geothermal Research**, [S.L.], v. 197, n. 1–4, p. 67-84, nov.2010. DOI: https://doi.org/10.1016/j.jvolgeores.2009.08.002.

BUTLER, R.; LAY, T.; CREAGER, K.; EARL, P.; FISCHER, K.; GAHERTY, J.; LASKE, G.; LEITH, B.; PARK, J.; RITZWOLLE, M.; TROMP, J.; WEN L. The global seismographic network surpasses its design goal. **Eos, Transactions American Geophysical Union**, [S.L.], v. 85, n. 23, p. 225–229, jun. 2004. DOI: https://doi.org/10.1029/2004EO230001.

CALÒ, M. Tears, windows, and signature of transform margins on slabs. Images of the Cocos plate fragmentation beneath the Tehuantepec isthmus (Mexico) using Enhanced Seismic Models. **Earth and Planetary Science Letters**, [S.L.], v. 560, n, 116788, p. 1-12, apr. 2021. DOI: https://doi.org/10.1016/j.epsl.2021.116788.

CAMPA, M. F.; CONEY, P. J. Tectono-stratigraphic terranes and mineral resource distributions of Mexico. **Canadian Journal of Earth Sciences**, [S.L.], v. 20, n. 6, p. 1040-1051, jun. 1983. DOI: https://doi.org/10.1139/e83-094.

CASTILLO, M. Landscape response to tectonics in sonora river basin (NW Mexico) using topographic and stream profile analysis. **Journal of South American Earth Sciences**, [S.L.], v. 111, n. 103446, p. 1–19, nov. 2021. DOI: https://doi.org/10.1016/j.jsames.2021.103446.

CASTILLO, M.; MUÑOZ-SALINAS, E.; FERRARI, L. Response of a landscape to tectonics using channel steepness indices (ksn) and OSL: A case of study from the Jalisco Block, Western Mexico. **Geomorphology**, [S.L.], v. 221, p. 204-214, sep. 2014. DOI: https://doi.org/10.1016/j.geomorph.2014.06.017.

CASTILLO-RODRÍGUEZ, M.; LÓPEZ-BLANCO, J.; MUÑOZ-SALINAS, E. A geomorphologic GIS-multivariate analysis approach to delineate environmental units, a case study of La Malinche volcano (central México). **Applied Geography**, v. 30, n. 4, p. 629-638, apr. 2010. DOI: https://doi.org/10.1016/j.apgeog.2010.01.003.

CORTINA C. Z. G.; WIGLEY, R.; PE'ERI, S. The GEBCO and NOAA Chart Adequacy Workshop. **Abstracts of International Cartographic Association**, [S.L.], v. 1, n. 51, p. 1, jul. 2019. DOI: https://doi.org/10.5194/ica-abs-1-51-2019.

EMAG2. Earth Magnetic Anomaly Grid (2-arc-minute resolution). Disponível em: https://catalog.data.gov/dataset/emag2-earth-magnetic-anomaly-grid-2-arc-minute-resolution. 2009. Acesso em: 03 dez. 2021.

FERRARI, L.; ESQUIVEL, T.; MANEA, V.; MANEA, M. The dynamic history of the Trans-Mexican Volcanic Belt and the Mexico subduction zone. **Tectonophysics**. [S.L.], v. 522–523, p. 122–149, oct. 2012. DOI: https://doi.org/10.1016/j.tecto.2011.09.018.

FITZ-DÍAZ, E.; LAWTON, T. F.; JUÁREZ-ARRIAGA, E.; CHÁVEZ-CABELLO, G. The Cretaceous-Paleogene Mexican orogen: Structure, basin development, magmatism and tectonics. **Earth-Science Reviews**, [S.L.], v. 183, p. 56-84, aug. 2018. DOI: https://doi.org/10.1016/j.earscirev.2017.03.002.

GARCÍA-SORIANO, D.; QUESADA-ROMÁN, A.; ZAMORANO-OROZCO, J. J. Geomorphological hazards susceptibility in high-density urban areas: A case study of Mexico City. **Journal of South American Earth Sciences**, [S.L.], v. 102, p. 102667, oct. 2020. DOI: https://doi.org/10.1016/j.jsames.2020.102667.

GAUGER, S., KUHN, G., GOHL, K., FEIGL, T., LEMENKOVA, P., HILLENBRAND, C. Swath-bathymetric mapping. **Reports on Polar and Marine Research**, [S.L.], v. 557, p. 38–45, 2007. DOI: https://doi.org/10.6084/m9.figshare.7439231.

GEBCO COMPILATION GROUP. **GEBCO 2020 Grid**. National Oceanography Centre: British Oceanographic Data Centre BODC, 2020. Disponível em: https://doi.org/10.5285/a29c5465-b138-234d-e053-6c86abc040b9. Acesso em: 26 jan. 2022.

GUILBAUD, M.-N.; HERNÁNDEZ-JIMÉNEZ, A.; SIEBE, C.; SALINAS, S. Las Cabras volcano, Michoacán-Guanajuato Volcanic Field, México: Topographic, climatic, and shallow magmatic

controls on scoria cone eruptions. **Revista Mexicana de Ciencias Geológicas**, [S.L.], v. 38, n. 2, p. 101-121, jul. 2021. DOI: https://doi.org/10.22201/cgeo.20072902e.2021.2.1645.

GODÍNEZ-DOMÍNGUEZ, E. A.; TENA-COLUNGA, A.; PÉREZ-ROCHA, L. E.; ARCHUNDIA-ARANDA, H. I.; GÓMEZ-BERNAL, A.; RUIZ-TORRES, R. P.; ESCAMILLA-CRUZ, J. L. The September 7, 2017 Tehuantepec, Mexico, earthquake: Damage assessment in masonry structures for housing. **International Journal of Disaster Risk Reduction**, [S.L.], v. 56, n. 102123, p. 1-31, apr. 2021. DOI: https://doi.org/10.1016/j.ijdrr.2021.102123.

GODÍNEZ-TAMAY, A.; CASTILLO, M.; FERRARI, L.; ORTEGA-GUTIÉRREZ, F. Assessing landscape response to tectonics in the Jalisco block and adjacent areas (west-central Mexico) using topographic analysis. **Journal of South American Earth Sciences**, [S.L.], v. 98, n. 102469, p.1-16, jan. 2020. DOI: https://doi.org/10.1016/j.jsames.2019.102469.

GOHL, K.; UENZELMANN-NEBEN, G.; EAGLES, G.; FAHL, A.; FEIGL, T.; GROBYS, J.; JUST, J.; LEINWEBER, V.; LENSCH, N.; MAYR, C.; PARSIEGLA, N.; RACKEBRANDT, N.; SCHLÜTER, P.; SUCKRO, S.; ZIMMERMANN, K.; GAUGER, S.; BOHLMANN, H.; NETZEBAND, G.; LEMENKOVA, P. Crustal and Sedimentary Structures and Geodynamic Evolution of the West Antarctic Continental Margin and Pine Island Bay. **Expeditionsprogramm Nr. 75 ANT XXIII/4 ANT XXIII/5**, 11–12, 2006. DOI: https://doi.org/10.13140/RG.2.2.16473.36961.

GÓMEZ-TUENA, A.; MORI, L.; STRAUB, S. M. Geochemical and petrological insights into the tectonic origin of the Transmexican Volcanic Belt. **Earth-Science Reviews**, v. 183, p. 153-181, aug. 2018. DOI: https://doi.org/10.1016/j.earscirev.2016.12.006.

GÓMEZ-VASCONCELOS, M. G.; AVELLÁN, D. R.; SORIA-CABALLERO, D.; MACÍAS, J. L.; VELÁZQUEZ-BUCIO, M. M.; JIMÉNEZ-HARO, A.; ISRADE-ALCÁNTARA, I.; GARDUÑO-MONROY, V. H.; ÁVILA-OLIVERA, J. A.; FIGUEROA-SOTO, Á. G.; CISNEROS-MÁXIMO, G.; CARDONA-MELCHOR, S. Geomorphic characterization of faults as earthquake sources in the Cuitzeo Lake basin, central México. **Journal of South American Earth Sciences**, [S.L.], v. 109, n. 103196, p. 1–16, aug. 2021. DOI: https://doi.org/10.1016/j.jsames.2021.103196.

GRAHAM, R.; PINDELL, J.; VILLAGÓMEZ, D.; MOLINA-GARZA, R.; GRANATH, J.; SIERRA-ROJAS, M. Integrated Cretaceous–Cenozoic plate tectonics and structural geology in southern Mexico. **Geological Society, London, Special Publications**, [S.L.], v. 504, p. 285-314, sep. 2020. DOI: https://doi.org/10.1144/SP504-2020-70.

HELFFRICH, G. GEBCO digital atlas. **Terra Nova**, [S.L.], v. 8, n. 6, p. 659-661, nov. 1996. DOI: https://doi.org/10.1111/j.1365-3121.1996.tb00795.x.

HOFMANN-WELLENHOF, B.; LICHTENEGGER, H.; COLLINS, H. J. Global Positioning System. New York: Springer-Verlag Wien, 1993.

JARA, J. M.; HERNÁNDEZ, E. J.; OLMOS, B. A.; MARTÍNEZ, G. Building damages during the September 19, 2017 earthquake in Mexico City and seismic retrofitting of existing first soft-story buildings. **Engineering Structures**, [S.L.], v. 209, n. 109977, p. 1-15, apr. 2020. DOI: https://doi.org/10.1016/j.engstruct.2019.109977.

JIMÉNEZ, C. Seismic source characteristics of the intraslab 2017 Chiapas-Mexico earthquake (Mw8.2). **Physics of the Earth and Planetary Interiors**, [S.L.], v. 280, p. 69-75, jul. 2018. DOI: https://doi.org/10.1016/j.pepi.2018.04.013.

KEPPIE, J. D.; DOSTAL, J.; NORMAN, M.; URRUTIA-FUCUGAUCHI, J.; GRAJALES-NISHIMURA, M. Study of melt and a clast of 546 Ma magmatic arc rocks in the 65 Ma Chicxulub bolide breccia, northern Maya block, Mexico: western limit of Ediacaran arc peripheral to northern Gondwana. **International Geology Review**, v. 53, n. 10, p. 1180-1193, jun. 2011. DOI: https://doi.org/10.1080/00206810903545527.

KLAUČO, M.; GREGOROVÁ, B.; STANKOV, U.; MARKOVIĆ, V.; LEMENKOVA, P. Determination of ecological significance based on geostatistical assessment: a case study from the Slovak Natura 2000 protected area. **Open Geosciences**, [S.L.], v. 5, n. 1, p. 28–42, mar. 2013. DOI: https://doi.org/10.2478/s13533-012-0120-0.

KLAUČO, M.; GREGOROVÁ, B.; KOLEDA, P.; STANKOV, U.; MARKOVIĆ, V.; LEMENKOVA, P. Land planning as a support for sustainable development based on tourism: A case study of Slovak Rural Region. **Environmental Engineering and Management Journal**, [S.L.], v. 16, n. 2, p. 449–458, feb. 2017. DOI: https://doi.org/10.30638/eemj.2017.045.

KUHN, G., HASS, C., KOBER, M., PETITAT, M., FEIGL, T., HILLENBRAND, C. D., KRUGER, S., FORWICK, M., GAUGER, S., LEMENKOVA, P. **The response of quaternary climatic cycles in the South-East Pacific:** development of the opal belt and dynamics behavior of the West Antarctic ice sheet. In: GOHL, K. (ed). Expeditionsprogramm n. 75 ANT XXIII/4, p. 12–13, jan. 2006. DOI: https://doi.org/10.13140/RG.2.2.11468.87687.

LAVIE, T.; ORON-GILAD, T.; MEYER, J. Aesthetics and usability of in-vehicle navigation displays. **International Journal of Human-Computer Studies**, [S.L.], v. 69, n. 1–2, p. 80-99, jan./feb. 2011. DOI: https://doi.org/10.1016/j.ijhcs.2010.10.002.

LEMENKOV, V.; LEMENKOVA, P. Measuring Equivalent Cohesion Ceq of the Frozen Soils by Compression Strength Using Kriolab Equipment. **Civil and Environmental Engineering Reports**, [S.L.], v. 31, n. 2, p. 63–84, jun. 2021a. DOI: https://doi.org/10.2478/ceer-2021-0020.

LEMENKOV, V.; LEMENKOVA, P. Using TeX Markup Language for 3D and 2D Geological Plotting. **Foundations of Computing and Decision Sciences**, [S.L.], v. 46, n. 3, p. 43–69, feb. 2021b. DOI: https://doi.org/10.2478/fcds-2021-0004.

LEMENKOVA, P. Geophysical Modelling of the Middle America Trench using GMT. **Annals of Valahia University of Targoviste. Geographical Series**, [S.L.], v. 19, n. 2, p. 73–94, 2019a. DOI: https://doi.org/10.6084/m9.figshare.12005148.

LEMENKOVA, P. Geomorphological modelling and mapping of the Peru-Chile Trench by GMT. **Polish Cartographical Review**, [S.L.], v. 51(4), p. 181–194, jan. 2019b. DOI: https://doi.org/10.2478/pcr-2019-0015.

LEMENKOVA, P. Topographic surface modelling using raster grid datasets by GMT: example of the Kuril-Kamchatka Trench, Pacific Ocean. **Reports on Geodesy and Geoinformatics**, [S.L.], v. 108, n.1, p. 9–22, nov. 2019c. DOI: https://doi.org/10.2478/rgg-2019-0008.

LEMENKOVA, P. Geomorphology of the Puerto Rico Trench and Cayman Trough in the Context of the Geological Evolution of the Caribbean Sea. **Annales Universitatis Mariae Curie-Sklodowska, sectio B – Geographia, Geologia, Mineralogia et Petrographia**, [S.L.], v. 75, p. 115-141, nov. 2020a. DOI: https://doi.org/10.17951/b.2020.75.115-141.

LEMENKOVA, P. GEBCO Gridded Bathymetric Datasets for Mapping Japan Trench Geomorphology by Means of GMT Scripting Toolset. **Geodesy and Cartography**, [S.L.], v. 46, n. 3, p. 98–112, oct. 2020b. DOI: https://doi.org/10.3846/gac.2020.11524.

LEMENKOVA, P. NOAA Marine Geophysical Data and a GEBCO Grid for the Topographical Analysis of Japanese Archipelago by Means of GRASS GIS and GDAL Library. **Geomatics and Environmental Engineering**, [S.L.], v. 14, n. 4, p. 25–45, nov. 2020c. DOI: https://doi.org/10.7494/geom.2020.14.4.25.

LEMENKOVA, P. GRASS GIS for topographic and geophysical mapping of the Peru-Chile Trench. **Forum Geografic**, [S.L.], v. 19, n. 2, p. 143–157, dec. 2020d. DOI: https://doi.org/10.5775/fg.2020.009.d.

LEMENKOVA, P. The visualization of geophysical and geomorphologic data from the area of Weddell Sea by the Generic Mapping Tools. **Studia Quaternaria**, [S.L.], v. 38, n. 1, p. 19–32, jan. 2021a. DOI: https://doi.org/10.24425/sq.2020.133759.

LERNER, J.; DENÈGRET, J.; MOORE, A. **Chapter 4 – Design and Semiology for Cartographic Representation**. *In*: DENÈGRE, J. (Ed.). Thematic Mapping from Satellite Imagery: a Guidebook. Pergamon, 1994, p. 63–72. DOI: https://doi.org/10.1016/B978-0-08-042351-7.50016-1.

LINDH, P.; LEMENKOVA, P. Evaluation of Different Binder Combinations of Cement, Slag and CKD for S/S Treatment of TBT Contaminated Sediments. **Acta Mechanica et Automatica**, [S.L.], v. 15, n. 4, p. 236–248, nov. 2021a. DOI: https://doi.org/10.2478/ama-2021-0030.

LINDH, P.; LEMENKOVA, P. Resonant Frequency Ultrasonic P-Waves for Evaluating Uniaxial Compressive Strength of the Stabilized Slag–Cement Sediments. **Nordic Concrete Research**, [S.L.], v. 65, n. 2, p. 39–62, dec. 2021b. DOI: https://doi.org/10.2478/ncr-2021-0012.

LOZANO-GARCÍA, D. F.; SANTIBAÑEZ-AGUILAR, J. E.; LOZANO, F. J.; FLORES-TLACUAHUAC, A. GIS-based modeling of residual biomass availability for energy and production in Mexico. **Renewable and Sustainable Energy Reviews**, [S.L.], v. 120, n. 109610, p. 1-16, mar. 2020. DOI: https://doi.org/10.1016/j.rser.2019.109610.

MAYA-MONDRAGÓN, J.; SÁNCHEZ-ROMÁN, F. R.; PALMA-ZARCO, A.; AGUILAR-SOTO, M.; BORJA-ABURTO, V. H. Prevalence of Post-traumatic Stress Disorder and Depression After the September 19th, 2017 Earthquake in Mexico. **Archives of Medical Research**, [S.L.], v. 50, n. 8, p. 502-508, nov. 2019. DOI: https://doi.org/10.1016/j.arcmed.2019.11.008.

MAUS, S.; BARCKHAUSEN, U.; BERKENBOSCH, H.; BOURNAS, N.; BROZENA, J.; CHILDERS, V.; DOSTALER, F.; FAIRHEAD, J. D.; FINN, C.; VON FRESE, R. R. B.; GAINA, C.; GOLYNSKY, S.; KUCKS, R.; LÜHR, H.; MILLIGAN, P.; MOGREN, S.; MÜLLER, R. D.; OLESEN, O.; PILKINGTON, M.; SALTUS, R.; SCHRECKENBERGER, B.; THÉBAULT, E.; CARATORI TONTINI, F. EMAG2: A 2–arc min resolution Earth Magnetic Anomaly Grid compiled

from satellite, airborne, and marine magnetic measurements. **Geochemistry, Geophysics, Geosystems**, v. 10, n. 8, p. 1-12, aug. 2009. DOI: https://doi.org/10.1029/2009GC002471.

MCMICHAEL-PHILLIPS, J. The Nippon Foundation-GEBCO Seabed 2030 Project: The Most Ambitious Seafloor Mapping Initiative in History. **Marine Technology Society Journal**, [S.L.], v. 55, n. 3, p. 25-28, mai./jun. 2021. DOI: https://doi.org/10.4031/MTSJ.55.3.3.

MEYER, B.; SALTUS, R.; CHULLIAT, A. EMAG2v3: Earth Magnetic Anomaly Grid (2-arc-minute resolution). Version 3. **NOAA National Centers for Environmental Information**, 2017. DOI: https://doi.org/10.7289/V5H70CVX. [Accessed: 07 August 2021].

MONTGOMERY, J.; CANDIA, G.; LEMNITZER, A.; MARTINEZ, A. The September 19, 2017 Mw 7.1 Puebla-Mexico City earthquake: Observed rockfall and landslide activity. **Soil Dynamics and Earthquake Engineering**, **[**S.L.], v. 130, n. 105972, p. 1-6, mar. 2020. DOI: https://doi.org/10.1016/j.soildyn.2019.105972.

MORA-KLEPEIS, G. Mexico and the Gulf of Mexico. *In*: ELIAS, S.; ALDERTON, D. (ed.). **Encyclopedia of Geology.** 2. ed. [S.L.]: Academic Press, 2021. p. 68-79. **DOI:** https://doi.org/10.1016/B978-0-08-102908-4.00138-7.

MOREHART, C. T. Mapping ancient chinampa landscapes in the Basin of Mexico: a remote sensing and GIS approach. **Journal of Archaeological Science**, v. 39, n. 7, p. 2541-2551, 2012. DOI: https://doi.org/10.1016/j.jas.2012.03.001.

ORTEGA-GUTIÉRREZ, F.; GÓMEZ-TUENA, A. Tectonic Systems of Mexico: Origin and Evolution. **Earth-Science Reviews**, **[**S.L.], v. 183, p. 1, aug. 2018. DOI: https://doi.org/10.1016/j.earscirev.2018.06.002.

ORTEGA-GUTIÉRREZ, F.; ELÍAS-HERRERA, M.; MORÁN-ZENTENO, D. J.; SOLARI, L.; WEBER, B.; LUNA-GONZÁLEZ, L. The pre-Mesozoic metamorphic basement of Mexico, 1.5 billion years of crustal evolution. **Earth-Science Reviews**, **[**S.L.], v. 183, p. 2-37, aug. 2018. DOI: https://doi.org/10.1016/j.earscirev.2018.03.006.

PADILLA Y SÁNCHEZ, R. J.; DOMÍNGUEZ TREJO, I.; LÓPEZ AZCÁRRAGA, A. G.; MOTA NIETO, J.; FUENTES MENES, A. O.; ROSIQUE NARANJO, F.; GERMÁN CASTELÁN, E. A.; CAMPOS ARRIOLA, S. E. **Tectonic Map of Mexico GIS Project**. American Association of Petroleum Geologists GIS Open Files series: National Autonomous University of Mexico: 2013.

PAVLIS, N. K.; HOLMES, S.; KENYON, S. C.; FACTOR, J. K. The development and evaluation of the Earth Gravitational Model 2008 (EGM2008). **Journal of Geophysical Research**, **[**S.L.], v. 117, n. B04406, p. 1-38, apr. 2012. DOI: https://doi.org/10.1029/2011JB008916.

RODRÍGUEZ-PÉREZ, Q.; RAMÓN ZUÑIGA, F. Imaging b-value depth variations within the Cocos and Rivera plates at the Mexican subduction zone. **Tectonophysics**, [S.L.], v. 734–735, p. 33-43, jun. 2018. DOI : https://doi.org/10.1016/j.tecto.2018.03.019.

RODRÍGUEZ-ZURRUNERO, A.; GRANJA-BRUÑA, J. L.; CARBÓ-GOROSABEL, A.; MUÑOZ-MARTÍN, A.; GOROSABEL-ARAUS, J. M.; GÓMEZ DE LA PEÑA, L.; GÓMEZ BALLESTEROS, M.; PAZOS, A.; CATALÁN, M.; ESPINOSA, S.; DRUET, M.; LLANES, P.; TEN BRINK, U. Submarine morpho-structure and active processes along the North American-

Caribbean plate boundary (Dominican Republic sector). **Marine Geology**, **[**S.L.], v. 407, p. 121-147, jan. 2019. DOI: https://doi.org/10.1016/j.margeo.2018.10.010.

SANDWELL, D. T., MÜLLER, R. D., SMITH, W. H. F., GARCIA, E., FRANCIS, R. New global marine gravity model from CryoSat-2 and Jason-1 reveals buried tectonic structure. **Science**, [S.L.], v. 7346 n. 6205, p. 65–67, oct. 2014. DOI: https://doi.org/10.1126/science.1258213.

SANTOS-REYES, J.; GOUZEVA, T. Mexico city's residents emotional and behavioural reactions to the 19 September 2017 earthquake. **Environmental Research**, **[**S.L.], v. 186, n. 109482, p. 1-11, jul. 2020. DOI: https://doi.org/10.1016/j.envres.2020.109482.

SCHENKE, H. W.; LEMENKOVA, P. Zur Frage der Meeresboden-Kartographie: Die Nutzung von AutoTrace Digitizer für die Vektorisierung der Bathymetrischen Daten in der Petschora-See. **Hydrographische Nachrichten**, **[**S.L.], v. 81, p. 16–21, jan. 2008. DOI: https://doi.org/10.6084/m9.figshare.7435538.

SCHENKE, H. General Bathymetric Chart of the Oceans (GEBCO). *In*: Harff J., Meschede M., Petersen S., Thiede J. (eds.) **Encyclopedia of Marine Geosciences**. Encyclopedia of Earth Sciences Series. Springer, Dordrecht, 2016. DOI: https://doi.org/10.1007/978-94-007-6238-1_63.

SOLARI, L. A.; GARCÍA-CASCO, A.; MARTENS, U.; LEE, J. K. W.; ORTEGA-RIVERA, A. Late Cretaceous subduction of the continental basement of the Maya block (Rabinal Granite, central Guatemala): Tectonic implications for the geodynamic evolution of Central America. **GSA Bulletin**, **[**S.L.], v. 125, n. 3-4, p. 625–639, mar. 2013. DOI: https://doi.org/10.1130/B30743.1.

SPIKINGS, R.; COCHRANE, R.; VILLAGOMEZ, D.; VAN DER LELIJ, R.; VALLEJO, C.; WINKLER, W.; BEATE, B. The geological history of northwestern South America: from Pangaea to the early collision of the Caribbean Large Igneous Province (290–75Ma). **Gondwana Research**, **[**S.L.], v. 27, n. 1, p. 95-139, jan. 2015. DOI: https://doi.org/10.1016/j.gr.2014.06.004.

SUETOVA, I.; USHAKOVA, L.; LEMENKOVA, P. Geoecological Mapping of the Barents Sea Using GIS. In: International Cartographic Conference., 22., 2005, A Coruña. **Anales [...].** A Coruña: International Cartographic Association (Ica), 2005a. DOI: https://doi.org/10.6084/m9.figshare.7435529.

SUETOVA, I. A.; USHAKOVA, L. A.; LEMENKOVA, P. Geoinformation mapping of the Barents and Pechora Seas. **Geography and Natural Resources**, **[**S.L.], v. 4, p. 138–142, 2005b. DOI: https://doi.org/10.6084/m9.figshare.7435535.

TAYLOR, R. M. Colour design in aviation cartography. **Displays**, **[**S.L.], v. 6, n. 4, p. 187-201, oct. 1985. DOI: https://doi.org/10.1016/0141-9382(85)90124-6.

TENA-COLUNGA, A. Conditions of structural irregularity. Relationships with observed earthquake damage in Mexico City in 2017. **Soil Dynamics and Earthquake Engineering**, **[**S.L.], v. 143, n. 106630, p. 1-29, apr. 2021. DOI: https://doi.org/10.1016/j.soildyn.2021.106630.

THYNG, K. M.; GREENE, C. A.; HETLAND, R. D.; ZIMMERLE, H. M.; DIMARCO, S. F. True colors of oceanography: Guidelines for effective and accurate colormap selection. **Oceanography**, **[**S.L.], v. 29, n. 3, p. 9–13, aug. 2016. DOI: https://doi.org/10.5670/oceanog.2016.66.

VÁZQUEZ, R.; MACÍAS, J. L.; ARCE, J. L. Integrated hazards maps of the Tacaná Volcanic complex, Mexico-Guatemala: Ashfall, block-and-ash flows, and lahars. **Journal of South American Earth Sciences**, **[**S.L.], v. 107, n. 103146, p. 1-11, apr. 2021. DOI: https://doi.org/10.1016/j.jsames.2020.103146.

WESSEL, P.; LUIS, J. F.; UIEDA, L.; SCHARROO, R.; WOBBE, F.; SMITH, W. H. F.; TIAN, D. The Generic Mapping Tools version 6. **Geochemistry, Geophysics, Geosystems**, [S.L.], v. 20, p. 5556–5564, sep. 2019. DOI: https://doi.org/10.1029/2019GC008515.